

The Reverse Quantum Limit: Implications for Unconventional Quantum Oscillations in YbB_{12}

Christopher A. Mizzi^{1*}, Satya K. Kushwaha^{1,2,3,4}, Priscila F.S. Rosa⁵, W. Adam Phelan^{3,4,6}, David C. Arellano⁶, Lucas A. Pressley^{2,3,7}, Tyrel M. McQueen^{2,3,7}, Mun K. Chan¹ and Neil Harrison^{1*}

¹National High Magnetic Field Laboratory, Los Alamos National Laboratory, Los Alamos, New Mexico, 87545, USA.

²Institute for Quantum Matter, William H. Miller III Department of Physics and Astronomy, The Johns Hopkins University, Baltimore, Maryland, 21218, USA.

³Department of Chemistry, The Johns Hopkins University, Baltimore, Maryland, 21218, USA.

⁴Platform for the Accelerated Realization, Analysis and Discovery of Interface Materials (PARADIM), Department of Chemistry, The Johns Hopkins University, Baltimore, Maryland, 21218, USA.

⁵MPA-Q, Los Alamos National Laboratory, Los Alamos, New Mexico, 87545, USA.

⁶MST-16, Los Alamos National Laboratory, Los Alamos, New Mexico, 87545, USA.

⁷Department of Materials Science and Engineering, The Johns Hopkins University, Baltimore, Maryland, 21218, USA.

*Corresponding author(s). E-mail(s): mizzi@lanl.gov; nharrison@lanl.gov;

Abstract

Beyond the quantum limit, many-body effects are expected to induce unusual electronic phase transitions. Materials possessing metallic ground states with strong interactions between localized and itinerant electronic states are natural candidates for the realization of such quantum phases. However, the electronic correlations responsible for increasing the likelihood of novel phases simultaneously place the quantum limit beyond the reach of laboratory magnets. Here we propose these difficulties can be surmounted in materials with strong correlations and insulating ground states. Strong correlations in insulators and high magnetic fields conspire to fill Landau levels in the reverse order compared to conventional metals, such that the lowest Landau level is the first observed. Consequently, the quantum limit in strongly correlated insulators is reached in reverse and at fields accessible in laboratories. Quantum oscillations measured at high fields in YbB_{12} are shown to have features consistent with the reverse quantum limit. These include how quantum oscillations move in lock step with the angular evolution of the insulator-metal transition and the field dependence of the quantum oscillation frequency. We argue that close to the insulator-metal transition, the insulating state should be viewed through the lens of a magnetic field-induced electronic instability affecting the lowest Landau level states in the quantum limit.

Keywords: Kondo Insulator, Quantum Oscillations, Quantum Limit, Insulator-Metal Transition

Large magnetic fields have dramatic effects on electron motion [1]. In metallic systems, these effects are particularly pronounced when the cyclotron energy exceeds the Fermi energy and electrons are confined to their lowest Landau level. The resulting ground state, often termed the quantum limit [2], is highly degenerate and susceptible to instabilities yielding a rich variety of electronic phases including spin- and charge-density waves, fractional quantum Hall states, and excitonic insulators [3–8]. The likelihood of such novel phases tends to increase with the strength of electronic correlations, which makes it extremely desirable to explore the quantum limit in metals with strong electronic correlations. f -electron metals are an enticing platform for such studies, however their large effective masses place the quantum limit beyond the reach of laboratory magnets [9–11]. Accordingly, quantum limit studies have largely focused on semimetals (*e.g.*, graphite [12, 13] and TaAs [14]) and two-dimensional systems (*e.g.*, graphene [15–17] and GaAs heterostructures [2]) where small effective masses and low carrier densities enable experimental access to the quantum limit.

In this paper, we propose the quantum limit in systems with strong electronic correlations is most readily reached in reverse, *i.e.*, from an insulating ground state. This “reverse quantum limit” occurs when the Zeeman energy exceeds the cyclotron energy in an insulator and results in reverse Landau level filling. First, we motivate the idea that the first Landau level crossing may correspond to

the lowest Landau level by presenting high-field measurements on the Kondo insulator YbB_{12} . We establish YbB_{12} as an ideal system to investigate reverse Landau level filling because it has (1) large Zeeman and small cyclotron energies, (2) a small gap (which sets a field scale amenable to laboratory magnets), and (3) reproducible high-field, low-temperature behavior (including unconventional quantum oscillations [20–22]). Then, we demonstrate the angular dependence of the quantum oscillations matches that of the insulator-metal transition field. To explain this observed pinning to the transition field, we formally introduce the reverse quantum limit and show this angular dependence and the field-dependent frequency of the quantum oscillations are manifestations of reverse Landau level filling. Lastly, we show the reverse quantum limit framework captures key aspects of the insulating state quantum oscillations, which suggests the insulating and metallic state quantum oscillations in YbB_{12} share a common origin.

YbB_{12} possesses small gaps of order meV at low temperatures (see SI [19]) arising from hybridization between conduction electrons and largely localized f -electrons [23]. When subjected to magnetic fields, YbB_{12} exhibits a large, negative magnetoresistance and undergoes a bulk insulator-metal transition (Fig. 1a). An Arrhenius analysis (Fig. 1b) indicates the insulator-metal transition is driven by field-induced gap closure [24] (Fig. 1c). At first, the activation gap

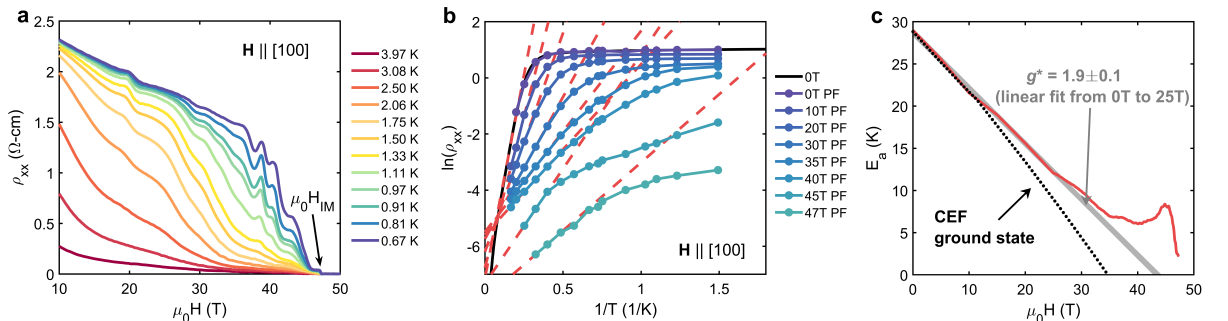


Fig. 1 (a) YbB_{12} in high magnetic fields exhibits substantial magnetoresistance, quantum oscillations, and a bulk insulator-metal transition (H_{IM}). (b) Arrhenius fits (red dashed lines) to the resistivity measured in pulsed fields (PF) were used to obtain the activation gap at fixed field values. The PF data are in good agreement with zero-field resistivity measurements (black). (c) The activation gap extracted in this manner (E_a , red) closes nearly linearly with field up to 25 T, consistent with Zeeman splitting-induced gap closure (grey line). Deviations from linear-in-field gap closure occur above 35 T prior to the insulator-metal transition and do not appear to be consistent with crystal electric field (CEF) level mixing (black, dotted). CEF data taken from Ref. [18]. See Supplementary Information for measurement and analysis details [19].

closes linearly with field, followed by notable deviations from linear gap closure above $\sim 35\text{T}$. The linear gap closure is consistent with Zeeman splitting of the conduction and valence band edges corresponding to $g^* = 1.9 \pm 0.1$ [25] (Fig. 1c). One possibility is that the high-field behavior may be related to crystal field level mixing [26]. However, the predicted crystal field ground state has an effective g factor which is too large to explain our observations [18, 27]. It is also possible the non-monotonic behavior is evidence of an excitonic insulator, a possibility that will be explored in greater detail later. Note, the zero field gap, transition field, and effective g factor reported here are consistent with other measurements on high-quality YbB_{12} single crystals [18, 20, 24, 28].

Magnetoresistance oscillations are present in the insulating state of YbB_{12} for $\mu_0 H \gtrsim 35\text{T}$ (Fig. 1a and Fig. 2a). The insulating state oscillations are periodic in inverse field with a dominant frequency $\sim 700\text{T}$. Frequencies were determined by indexing maxima and minima of the oscillations and then either finding the slope with respect to inverse field (insulating state) or computing finite differences (metallic state); see Supplementary Information for additional details [19]. Temperature dependent amplitudes are consistent with the Lifshitz-Kosevich (LK) form ($m^* \approx 7.6m_e$, see SI [19]), which suggests these insulating oscillations are Shubnikov-de Haas (SdH) quantum oscillations [29]. SdH quantum oscillations in the field-induced metallic state (Fig. 2b) were observed using tunnel-diode oscillator (TDO) measurements, which are a contactless resistance method [30]. The metallic state quantum oscillations possess a field-dependent frequency (Fig. 2c) and, like the insulating state oscillations, have temperature dependent amplitudes described by the LK equation. Fitting with the LK equation indicates the metallic state effective mass is large ($\sim 10m_e$), increases with field, and has little anisotropy (see SI [19]). Importantly, the quantum oscillations in Fig. 2 are in good agreement with previous reports in both the insulating [20, 31] and metallic states [21, 22] of YbB_{12} . This demonstrates quantum oscillations in high-quality YbB_{12} are a robust and reproducible phenomenon.

The onset of the field-induced metallic state is anisotropic, increasing when the direction of the

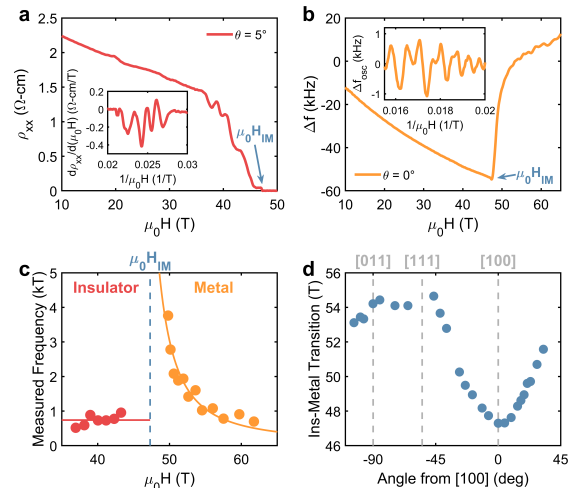


Fig. 2 (a) Magnetoresistance and (b) contactless resistance showing quantum oscillations in the insulating phase and metallic phase, respectively. Insets show (a) derivative of magnetoresistance and (b) background subtracted contactless resistance as functions of inverse field. (c) Insulating state quantum oscillations have a field-independent frequency of $740 \pm 60\text{T}$ and metallic state quantum oscillations have a field-dependent frequency ($\mathbf{H} \parallel [100]$). Lines are guides for the eye. (d) Angular dependence of the insulator-metal transition field (H_{IM}). All measurements were at $\sim 650\text{mK}$. Angles correspond to rotations in the [100]-[011] plane referenced to [100].

applied field is rotated away from [100] towards [011] ($H_{IM}^{[011]}/H_{IM}^{[100]} = 1.15$, Fig. 2d). We attribute this anisotropy to an anisotropic g^* , which is consistent with crystal field predictions [18]. For fields applied in the [100]-[011] plane, the angular dependence of the quantum oscillations measured at base temperature reveals that both the metallic and insulating state quantum oscillations indices follow the angular dependence of the insulator-metal transition; *i.e.*, the oscillations are pinned to the insulator-metal transition. Although there is some evolution in the fine structure of the oscillations, the dominant angular dependence of the oscillations matches the angular variation of the insulator-metal transition over a large angular and field range (Fig. 3). The relationship between the quantum oscillations and the insulator-metal transition is most clearly demonstrated by tracking both phenomena at different angles (Fig. 3c); the angular dependence of each quantum oscillation and the insulator-metal transition collapses to a single curve when referenced to values at $\mathbf{H} \parallel [100]$

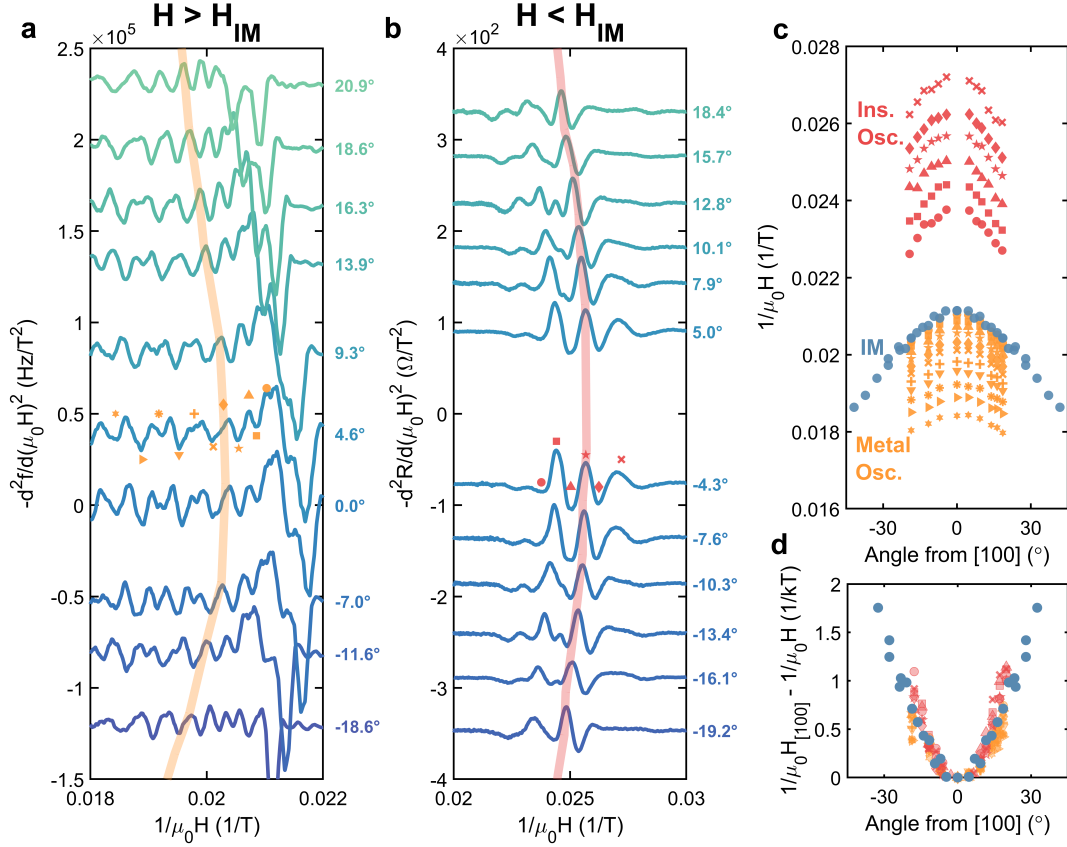


Fig. 3 Second derivatives of (a) contactless resistance and (b) magnetoresistance as functions of inverse field for fields applied in the [100]-[011] plane (0° corresponds to [100]). Data are vertically offset in proportion to angle from [100]. Maxima and minima of oscillations are denoted by symbols and lines are included as guides for the eye. Second derivatives were used to avoid artifacts stemming from background subtraction, and average positions were tracked in cases of split oscillations; see Supplementary Information for details [19]. (c) Tracking the angular evolution of individual oscillations (different symbols) in the metallic and insulating states and (d) referencing each to its value when $\mathbf{H} \parallel [100]$ demonstrates the angular dependence of quantum oscillations follows the insulator-metal transition for a large range of angles and fields in both the (a) metallic and (b) insulating states. All measurements were at ~ 650 mK.

(Fig. 3d). Therefore, the quantum oscillations are pinned to the insulator-metal transition.

To understand the surprising observation of Landau level indices that are tied to the metal-insulator transition, we contrast the behavior of Landau levels in a conventional metal with those of an insulator and, in doing so, introduce the reverse quantum limit. Electronic states in a conventional metal are quantized by a magnetic field into Landau levels [1, 29]. When Zeeman splitting is considered, the Landau levels are given by

$$E^{\uparrow,\downarrow} - \mu = \frac{\hbar e}{m^*} B \left(\nu + \frac{1}{2} \right) \mp \frac{1}{2} g^* \mu_B B, \quad (1)$$

where $E^{\uparrow,\downarrow}$ is the energy of the up/down ($-$, $+$) spin state referenced to the chemical potential μ , B is magnetic field ($B \approx \mu_0 H$ for the applied magnetic fields used in this work [21]), \hbar is Plank's constant, e is electron charge, m^* is effective mass, ν is the Landau level index, g^* is an effective g -factor (for pseudospins of $1/2$ that is renormalized by interactions), and μ_B is the Bohr magneton. Upon increasing field, Landau levels with decreasing indices sequentially cross the chemical potential. This process continues until the lowest Landau level is reached, corresponding to a conventional metal in the quantum limit (Fig. 4a).

Electron states in insulators are also quantized by magnetic fields, similar to the case described

by Eq. (1). For illustrative purposes, we assume a symmetric band structure with the chemical potential at the center of a zero-field gap (Δ). Note, factors such as disorder will reduce the activation gap (E_a , Fig. 1) from its thermodynamic value (Δ); see Fig. 6 for further clarification. Then, the conduction band edge (E_C) in the presence of a magnetic field is given by

$$E_C^{\uparrow,\downarrow} - \mu = \Delta + \frac{\hbar e}{m^*} B \left(\nu + \frac{1}{2} \right) \mp \frac{1}{2} g^* \mu_B B. \quad (2)$$

Landau level crossings ($E_C = \mu$) will only occur if the Zeeman energy exceeds the cyclotron energy, *i.e.* if $g^* \frac{m^*}{m_e} > 2$, where m_e is the bare electron

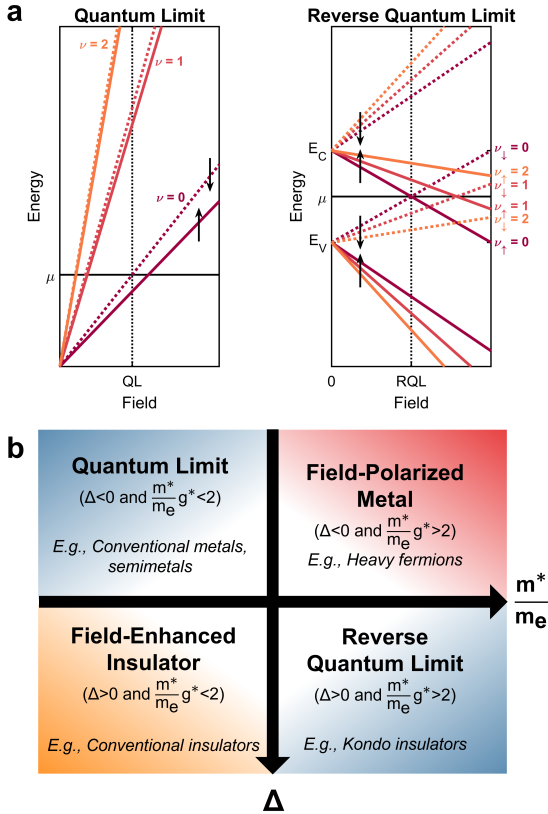


Fig. 4 (a) Landau level diagrams for the quantum limit (QL) and reverse quantum limit (RQL). A conventional metal reaches the QL when the cyclotron energy exceeds the Fermi energy. An insulator with a Zeeman energy greater than the cyclotron energy is similar, except the Landau levels cross the chemical potential in reverse. (b) High-field electronic phase diagram considering if the electronic structure at the chemical potential is gapped ($\Delta > 0$) or metallic ($\Delta < 0$), and the strength of electronic correlations ($g^* \frac{m^*}{m_e}$).

mass (see SI [19]). The quantity $g^* \frac{m^*}{m_e}$ can be considered a proxy for the strength of electronic correlations. When this condition is met, increasing the field causes Landau levels with increasing indices to sequentially cross the chemical potential such that the lowest Landau level is the first to cross (Fig. 4a). Therefore, the insulator is in the quantum limit at the first Landau level crossing. We call this the reverse quantum limit.

Another way to understand the reverse quantum limit is to consider the reverse quantum limit criterion, $g^* \frac{m^*}{m_e}$, in conjunction with the electronic structure at the chemical potential—gapped ($\Delta > 0$) or metallic ($\Delta < 0$). Together, $g^* \frac{m^*}{m_e}$ and Δ provide a means to classify materials according to their behavior in high magnetic fields (Fig. 4b). The quantum limit represents the most familiar case. It is realized in systems with light carriers (and/or small Zeeman energies), which have states at the chemical potential. If such a system were to be gapped it would behave as a field-enhanced insulator, whereas the introduction of stronger electronic correlations would yield a field-polarized metal. The remaining combination of $g^* \frac{m^*}{m_e}$ and Δ describes a system which is the reverse of the quantum limit, *i.e.*, gapped at the chemical potential with heavy carriers (and/or large Zeeman energies).

Returning to YbB_{12} , we find the experimentally determined Zeeman energy ($g^* = 1.9$) and effective mass ($m^* \sim 10m_e$) satisfy the reverse quantum limit criterion ($g^* \frac{m^*}{m_e} > 2$). Furthermore, Eq. (2) implies Landau level crossings occur when

$$\frac{1}{B_{IM}} - \frac{1}{B_\nu} = \frac{\hbar e}{\Delta m^*} \nu \quad (3)$$

where B_{IM} is the insulator-metal transition field and B_ν is the field at which Landau level ν crosses the chemical potential. Because the right-hand side of Eq. (3) only weakly depends on angle in the vicinity of the insulator-metal transition (see SI [19]), quantum oscillations are expected to be pinned to the insulator-metal transition in the reverse quantum limit, consistent with the data in Fig. 3.

Furthermore, Eq.(3) corresponds to a quantum oscillation frequency,

$$|F| = \frac{m^*}{\hbar e} \Delta, \quad (4)$$

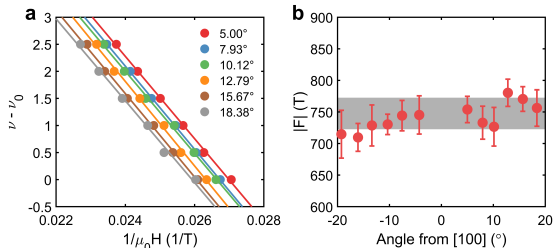


Fig. 5 (a) Landau level indices (ν) as a function of inverse field in the insulating state for the magnetic field applied along different angles with respect to [100]. Landau levels were indexed by tracking maxima and minima of the oscillations and are reported relative to the first observed oscillation. The indices follow the reverse quantum limit convention, *i.e.*, lower Landau levels occur at lower fields. Linear fits to the data (solid lines) show nearly identical slopes. (b) The quantum oscillation frequencies corresponding to the slopes in (a) show minimal variation with angle. All data was acquired at ~ 650 mK. Additional data provided in SI [19].

which is proportional to the product of the effective mass and hybridization gap. As both of these quantities exhibit little angular dependence (see SI [19]), the reverse quantum limit scenario predicts a quantum oscillation frequency which does not depend on angle. As shown in Fig. 5, the Landau level indices in the insulating state exhibit a linear relationship with inverse field characterized by a slope that varies minimally with angle, consistent with Landau levels filling in reverse.

The field-dependent quantum oscillation frequency (Fig. 2c) also arises naturally in the reverse quantum limit if the hybridization gap varies with field. If Δ becomes field-dependent in the metallic state, Eq. (2) implies the quantum oscillation frequency is

$$F(B) = \frac{m^*}{\hbar e} \left(B \frac{d\Delta(B)}{dB} - \Delta(B) \right), \quad (5)$$

where $\Delta(B)$ denotes the field-dependent gap. Thus, the quantum oscillation frequency can exhibit a non-linear field dependence if the gap in the metallic state is a non-linear function of field (see SI [19]). Similar considerations explain the slight deviations from the insulator-metal transition at higher angles in the metallic state in Fig. 3d (see SI [19]). Note, while Δ is a constant in the insulating state corresponding to the zero-field gap at the chemical potential, it is also related to the spacing between the zeroth Landau levels of

the conduction and valence bands for a given spin at finite field (Fig. 6a). Therefore, this quantity is well-defined in both the insulating and metallic states.

One possible origin for a non-linear $\Delta(B)$ is a situation in which the magnetic field alters the hybridization between conduction electrons and largely localized f -electrons [9, 32]. A scenario in which the hybridization gap is reduced by the applied field is consistent with the appearance of non-linear magnetization in the field-induced metallic state [18, 21, 24] owing to partial f -electron polarization: f -electron fluctuations are suppressed by f -electron polarization at high fields, which disrupts the Kondo-type mechanism responsible for the gap [32].

To formalize the connection between the gap and extent of f -electron polarization, *i.e.*, the non-linear portion of the magnetization in the high-field metallic state, we assume the Fermi surface area (A) is related to the non-linear component of the magnetization (M) through

$$A(B) = a \left(\frac{M(B)}{\mu_B} \right)^{2/3} \quad (6)$$

where a is a constant related to the degeneracy factor and the $2/3$ power arises from assuming ellipsoidal pockets (see SI [19]). With this assumption, the measured quantum oscillation frequency is

$$F_m = -B^2 \frac{d}{dB} \left[\frac{\hbar}{2\pi e} \frac{1}{B} a \left(\frac{M(B)}{\mu_B} \right)^{2/3} \right]. \quad (7)$$

As shown in Fig. 6, applying Eq. (7) yields good agreement between the field dependence of our measured quantum oscillation frequencies in the metallic state and literature values for the magnetization [21] with a single tunable parameter ($a \approx 3$). Fixing this a value also gives the field-dependence of the Landau indices and hybridization gap (see SI [19]). An example of the non-linear field-dependence of the Landau levels implied by Eq. (6) is depicted in Fig. 6a.

The above analysis shows the reverse quantum limit explains the quantum oscillations in the metallic state of YbB_{12} : the metallic quantum oscillations track the angular dependence of the insulator-metal transition because they arise

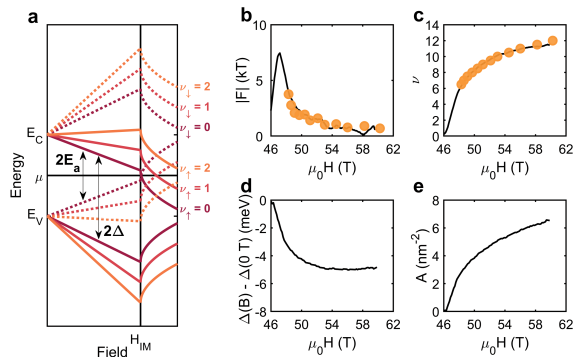


Fig. 6 (a) Landau level plot considering the combined effects of Zeeman splitting, Landau quantization, and gap reduction at high fields. Above the insulator-metal transition the Landau levels have a non-linear field dependence owing to the non-linear magnetization. (b) Quantum oscillation frequency (F) computed assuming the Fermi surface area is proportional to $M^{2/3}$ (black) compared to the measured quantum oscillation frequency in the metallic state (orange). From this relationship it is possible to determine the (c) Landau indices (ν) of the quantum oscillations and the field-dependence of the (d) gap ($\Delta(B) - \Delta(0T)$) and (e) Fermi surface area (A). Magnetization data is taken from Ref. [21].

from the Landau quantization of bulk bands in an insulator which has a Zeeman energy which exceeds the cyclotron energy, and they exhibit a field-dependent frequency owing to the reduction of the hybridization gap in the high-field metallic state. In other words, the Landau indexing and the insulator-to-(semi)metal transition are inextricably linked in the reverse quantum limit scenario; such a link would not exist were the carriers contributing to metallic conduction not from Landau-quantized states.

Moreover, the insulating state oscillations exhibit a similar connection to the insulator-metal transition (Fig. 3) which strongly suggests they are a bulk phenomenon and manifestations of the same bulk Landau levels responsible for the metallic state quantum oscillations. Using Eq. (4) with the measured mass and quantum oscillation frequency in the insulating state yields $\Delta \sim 8$ meV, which is larger than transport gaps (*e.g.*, Fig. 1), but consistent with optical gaps [33]. Since factors such as disorder can reduce the transport gap from its thermodynamic value, our reverse quantum limit interpretation suggests the oscillations in the insulating state are related to the thermodynamic gap.

The reverse quantum limit implies entry into the insulating regime with decreasing magnetic field (and entry into the metallic regime with increasing magnetic field) meets some of the pre-conditions for the realization of magnetic field-induced electronic instabilities [3–8]. One possibility is a transition to an excitonic insulator at high fields prior to the insulator-metal transition in analogy with other quantum limit systems like graphite [12, 13] and TaAs [14], but with much stronger electronic correlations. Such a transition is most likely to occur at the lowest Landau levels, *i.e.*, close to the insulator-metal transition, and would cause the insulator-metal transition to occur at a higher value of ν than 0. As our lowest observed Landau level in the metallic state appears to be $\nu \approx 7$ (Fig. 6), this is a possibility. Additionally, an excitonic insulator phase could gap the Landau levels in the (reverse) quantum limit [4], perhaps explaining the resistivity oscillations in the insulating phase at high fields. An excitonic transition would also explain the deviations from linear-in-field gap closure for $\mu_0 H \gtrsim 35$ T (Fig. 1c) and is consistent with the insulator-metal transition being first order [18, 34]. While we do not observe deviations from LK behavior (predicted for some scenarios with quantum oscillations arising in excitonic insulators [35–38]), these deviations may only be measurable at lower temperatures than were attainable in these experiments (see SI [19]).

There are currently numerous proposals for the origin of the unconventional, insulating state quantum oscillations in YbB₁₂ which invoke concepts such as charge-neutral Fermi surfaces [39–42] and non-Hermitian in-gap states [43]. Our work indicates a common set of bulk Landau levels drive the insulating and metallic oscillations; however, exactly how these Landau levels yield resistivity oscillations while the bulk remains electrically insulating remains to be addressed. Future work will be needed to understand the consequences of the reverse quantum limit on alternative proposals.

In summary, we have introduced a quantum limit analogue in insulators, the reverse quantum limit, which occurs when the Zeeman energy exceeds the cyclotron energy. The Kondo insulator YbB₁₂ is an ideal system to observe this phenomenon because it possesses an electronic structure which satisfies the reverse quantum limit

criterion while having an exceptionally small gap which can be closed by fields accessible in the laboratory. Predictions from the reverse quantum limit model are shown to explain how quantum oscillations are pinned to the insulator-metal transition and have a field-dependent frequency in the metallic state. While a detailed mechanism for the insulating state quantum oscillations remains elusive, our work suggests they originate from the same bulk Landau levels as the metallic quantum oscillations, and provides important empirical benchmarks for theoretical descriptions of quantum oscillations in YbB_{12} by demonstrating the central role of the insulator-metal transition.

Acknowledgments. This work was supported by the Department of Energy (DOE) Basic Energy Sciences (BES) project “Science of 100 Tesla.” The National High Magnetic Field Laboratory is funded by National Science Foundation (NSF) Cooperative Agreements No. DMR-1157490 and No. 1164477, the State of Florida, and DOE. C.A.M. and M.K.C. were supported by the LANL LDRD Program, Project No. 20210320ER. M.K.C. acknowledges support from NSF IR/D program while serving at the National Science Foundation. Any opinion, findings, and conclusions or recommendations expressed in this material are those of the author(s) and do not necessarily reflect the views of the National Science Foundation. S.K.K. acknowledges support of the LANL Directors Postdoctoral Funding LDRD program. This work made use of the synthesis facility of the Platform for the Accelerated Realization, Analysis, and Discovery of Interface Materials (PARADIM), which is supported by the NSF under Cooperative Agreement No. DMR-2039380. Work at Johns Hopkins University was supported by the Institute for Quantum Matter, an Energy Frontier Research Center funded by DOE, Office of Science, BES under Award No. DE-SC0019331. Additional data related to the crystal growth is available at <https://doi.org/10.34863/xxxxx>. The authors thank Joe D. Thompson for performing the susceptibility measurements in the Supplementary Information and Boris Maiorov for helpful discussions.

References

- [1] Ashcroft, N. & Mermin, N. *Solid State Physics* (Cengage Learning, 2011).
- [2] Tsui, D. C., Stormer, H. L. & Gossard, A. C. Two-Dimensional Magnetotransport in the Extreme Quantum Limit. *Phys. Rev. Lett.* **48**, 1559–1562 (1982). <https://doi.org/10.1103/PhysRevLett.48.1559> .
- [3] Fenton, E. W. Excitonic Insulator in a Magnetic Field. *Phys. Rev.* **170**, 816–821 (1968). <https://doi.org/10.1103/PhysRev.170.816> .
- [4] Yoshioka, D. & Fukuyama, H. Electronic Phase Transition of Graphite in a Strong Magnetic Field. *J. Phys. Soc. Japan* **50** (3), 725–726 (1981). <https://doi.org/10.1143/JPSJ.50.725> .
- [5] Halperin, B. I. Possible States for a Three-Dimensional Electron Gas in a Strong Magnetic Field. *Jpn. J. Appl. Phys.* **26** (S3-3), 1913 (1987). <https://doi.org/10.7567/JJAPS.26S3.1913> .
- [6] Fradkin, E. & Kivelson, S. A. Liquid-crystal phases of quantum hall systems. *Phys. Rev. B* **59**, 8065–8072 (1999). <https://doi.org/10.1103/PhysRevB.59.8065> .
- [7] Khveshchenko, D. V. Magnetic-Field-Induced Insulating Behavior in Highly Oriented Pyrolytic Graphite. *Phys. Rev. Lett.* **87**, 206401 (2001). <https://doi.org/10.1103/PhysRevLett.87.206401> .
- [8] Jain, J. K. *Composite Fermions* (Cambridge University Press, 2007).
- [9] Edwards, D. M. & Green, A. C. M. Heavy fermions in high magnetic fields. *Z. Phys. B* **103** (2), 243–249 (1996). <https://doi.org/10.1007/s002570050367> .
- [10] Altarawneh, M. M. *et al.* Sequential Spin Polarization of the Fermi Surface Pockets in URu_2Si_2 and Its Implications for the Hidden Order. *Phys. Rev. Lett.* **106**, 146403 (2011). <https://doi.org/10.1103/PhysRevLett.106.146403> .

- [11] Kushwaha, S. K. *et al.* Magnetic field-tuned Fermi liquid in a Kondo insulator. *Nature Communications* **10** (1), 5487 (2019). <https://doi.org/10.1038/s41467-019-13421-w> .
- [12] Iye, Y. *et al.* High-magnetic-field electronic phase transition in graphite observed by magnetoresistance anomaly. *Phys. Rev. B* **25**, 5478–5485 (1982). <https://doi.org/10.1103/PhysRevB.25.5478> .
- [13] Zhu, Z. *et al.* Graphite in 90 T: Evidence for Strong-Coupling Excitonic Pairing. *Phys. Rev. X* **9**, 011058 (2019). <https://doi.org/10.1103/PhysRevX.9.011058> .
- [14] Ramshaw, B. J. *et al.* Quantum limit transport and destruction of the Weyl nodes in TaAs. *Nat. Comm.* **9** (1), 2217 (2018). <https://doi.org/10.1038/s41467-018-04542-9> .
- [15] Geim, A. K. & Novoselov, K. S. The rise of graphene. *Nat. Mater.* **6** (3), 183–191 (2007). <https://doi.org/10.1038/nmat1849> .
- [16] Goerbig, M. O. Electronic properties of graphene in a strong magnetic field. *Rev. Mod. Phys.* **83**, 1193–1243 (2011). <https://doi.org/10.1103/RevModPhys.83.1193> .
- [17] Moon, P. & Koshino, M. Energy spectrum and quantum Hall effect in twisted bilayer graphene. *Phys. Rev. B* **85**, 195458 (2012). <https://doi.org/10.1103/PhysRevB.85.195458> .
- [18] Terashima, T. T. *et al.* Magnetization Process of the Kondo Insulator YbB_{12} in Ultra-high Magnetic Fields. *J. Phys. Soc. Japan* **86** (5), 054710 (2017). <https://doi.org/10.7566/JPSJ.86.054710> .
- [19] See supplementary information .
- [20] Xiang, Z. *et al.* Quantum oscillations of electrical resistivity in an insulator. *Science* **362** (6410), 65–69 (2018). <https://doi.org/10.1126/science.aap9607> .
- [21] Xiang, Z. *et al.* Unusual high-field metal in a Kondo insulator. *Nat. Phys.* **17** (7), 788–793 (2021). <https://doi.org/10.1038/s41567-021-01216-0> .
- [22] Liu, H. *et al.* f-electron hybridised Fermi surface in magnetic field-induced metallic YbB_{12} . *npj Quantum Mater.* **7** (1), 12 (2022). <https://doi.org/10.1038/s41535-021-00413-7> .
- [23] Riseborough, P. S. Heavy fermion semiconductors. *Adv. Phys.* **49** (3), 257–320 (2000). <https://doi.org/10.1080/000187300243345> .
- [24] Sugiyama, K., Iga, F., Kasaya, M., Kasuya, T. & Date, M. Field-Induced Metallic State in YbB_{12} under High Magnetic Field. *J. Phys. Soc. Japan* **57** (11), 3946–3953 (1988). <https://doi.org/10.1143/JPSJ.57.3946> .
- [25] The convention used throughout this work is $g^* = g_J m_J$.
- [26] Moll, P. J. W. *et al.* Emergent magnetic anisotropy in the cubic heavy-fermion metal CeIn_3 . *npj Quantum Materials* **2** (1), 46 (2017). <https://doi.org/10.1038/s41535-017-0052-5> .
- [27] Kurihara, R. *et al.* Field-induced valence fluctuations in YbB_{12} . *Phys. Rev. B* **103**, 115103 (2021). <https://doi.org/10.1103/PhysRevB.103.115103> .
- [28] Iga, F., Shimizu, N. & Takabatake, T. Single crystal growth and physical properties of kondo insulator YbB_{12} . *J. Magn. Magn. Mater.* **177-181**, 337–338 (1998). [https://doi.org/10.1016/S0304-8853\(97\)00493-9](https://doi.org/10.1016/S0304-8853(97)00493-9) .
- [29] Shoenberg, D. *Magnetic Oscillations in Metals* Cambridge Monographs on Physics (Cambridge University Press, 1984).
- [30] Coffey, T. *et al.* Measuring radio frequency properties of materials in pulsed magnetic fields with a tunnel diode oscillator. *Rev. Sci. Instrum.* **71** (12), 4600–4606 (2000). <https://doi.org/10.1063/1.1321301> .
- [31] Xiang, Z. *et al.* Hall Anomaly, Quantum Oscillations and Possible Lifshitz Transitions in Kondo Insulator YbB_{12} : Evidence for Unconventional Charge Transport. *Phys.*

- Rev. X* **12**, 021050 (2022). <https://doi.org/10.1103/PhysRevX.12.021050> .
- [32] Aoki, D., Knafo, W. & Sheikin, I. Heavy fermions in a high magnetic field. *Comptes Rendus Physique* **14** (1), 53–77 (2013). <https://doi.org/10.1016/j.crhy.2012.11.004> .
- [33] Okamura, H. *et al.* Indirect and Direct Energy Gaps in Kondo Semiconductor YbB_{12} . *J. Phys. Soc. Japan* **74** (7), 1954–1957 (2005). <https://doi.org/10.1143/JPSJ.74.1954> .
- [34] Iga, F. *et al.* Anisotropic magnetoresistance and collapse of the energy gap in $\text{Yb}_{1-x}\text{Lu}_x\text{B}_{12}$. *J. Phys. Conf. Ser.* **200** (1), 012064 (2010). <https://doi.org/10.1088/1742-6596/200/1/012064> .
- [35] Knolle, J. & Cooper, N. R. Quantum Oscillations without a Fermi Surface and the Anomalous de Haas–van Alphen Effect. *Phys. Rev. Lett.* **115**, 146401 (2015). <https://doi.org/10.1103/PhysRevLett.115.146401> .
- [36] Zhang, L., Song, X.-Y. & Wang, F. Quantum oscillation in narrow-gap topological insulators. *Phys. Rev. Lett.* **116**, 046404 (2016). <https://doi.org/10.1103/PhysRevLett.116.046404> .
- [37] Knolle, J. & Cooper, N. R. Excitons in topological kondo insulators: Theory of thermodynamic and transport anomalies in SmB_6 . *Phys. Rev. Lett.* **118**, 096604 (2017). <https://doi.org/10.1103/PhysRevLett.118.096604> .
- [38] He, W.-Y. & Lee, P. A. Quantum oscillation of thermally activated conductivity in a monolayer WTe_2 -like excitonic insulator. *Phys. Rev. B* **104**, L041110 (2021). <https://doi.org/10.1103/PhysRevB.104.L041110> .
- [39] Coleman, P., Miranda, E. & Tsvetlik, A. Odd-frequency pairing in the Kondo lattice. *Phys. Rev. B* **49**, 8955–8982 (1994). <https://doi.org/10.1103/PhysRevB.49.8955> .
- [40] Baskaran, G. Majorana Fermi Sea in Insulating SmB_6 : A proposal and a Theory of Quantum Oscillations in Kondo Insulators (2015). Preprint at <https://arxiv.org/abs/1507.03477>.
- [41] Chowdhury, D., Sodemann, I. & Senthil, T. Mixed-valence insulators with neutral Fermi surfaces. *Nat. Comm.* **9** (1), 1766 (2018). <https://doi.org/10.1038/s41467-018-04163-2> .
- [42] Sodemann, I., Chowdhury, D. & Senthil, T. Quantum oscillations in insulators with neutral Fermi surfaces. *Phys. Rev. B* **97**, 045152 (2018). <https://doi.org/10.1103/PhysRevB.97.045152> .
- [43] Shen, H. & Fu, L. Quantum Oscillation from In-Gap States and a Non-Hermitian Landau Level Problem. *Phys. Rev. Lett.* **121**, 026403 (2018). <https://doi.org/10.1103/PhysRevLett.121.026403> .